Vibrational Overtone Activation of the Isomerization of Methyl Isocyanide

Salah Hassoon, Nandani Rajapakse, and Deanne L. Snavely*

Center for Photochemical Sciences, Bowling Green State University, Bowling Green, Ohio 43403
(Received: September 15, 1991; In Final Form: November 26, 1991)

The photoisomerization of methyl isocyanide to form acetonitrile induced by excitation into the fourth (~1 kcal/mol above the activation barrier) and fifth (~8 kcal/mol above the barrier) C-H stretch vibrational overtones is reported. The ratio of the collisional deactivation rate constant to the unimolecular rate coefficient, $k(\epsilon)$, was determined by a Stern-Volmer analysis plotting the inverse apparent rate constant against the total pressure. The unimolecular rate coefficients increase monotonically with increasing excitation energies across the rotational band contours. The experimental $k(\epsilon)$ agree with RRKM calculated values. The Stern-Volmer plots are nonlinear at low pressure: the fourth overtone excitation shows negative curvature (decreasing slope with increasing pressure) and the fifth overtone shows positive curvature (increasing slope with increasing pressure). The magnitude and direction of this curvature agree with the calculated Stern-Volmer plots in earlier work using a master equation simulation. In these vibrational overtone activation studies, the collisional deactivation efficiency of argon is 0.3 of that of the self-collider.

Introduction

Vibrational overtone photoactivation has been used to study a number of gas-phase reactions in polyatomic molecules.[1,2] Highly excited vibrational states corresponding to local modes of the molecule are responsible for the absorption of light.[3-5] With this method, vibrational states lying 30-50 kcal/mol above the ground state can be pumped through the absorption of a single photon. The ratio of the collisional deactivation rate to the unimolecular rate coefficient can be obtained through the Stern-Volmer analysis of the overtone photoactivation experiment.

The unimolecular isomerization of methyl isocyanide (MIC) to form acetonitrile (AN) has long served as a prototype for unimolecular reaction studies. The thermal isomerization of MIC has been extensively investigated by Rabinovitch and co-workers.[6-8] Their experimental unimolecular rate constants were consistent with the statistical assumptions in RRKM theory.[9,10] In contrast, theoretical trajectory calculations for this reaction carried out by Bunker, Harris, and Hase[11-13] have shown non-RRKM behavior, which is a nonstatistical distribution of the energy on the time scale of the isomerization.

Reddy and Berry studied the laser-induced isomerization of MIC, using for the first time, a direct C-H stretch overtone excitation.[14-16] The reaction rate constants obtained from a Stern-Volmer treatment were higher than calculated RRKM rates, which fit the thermal data.[6] The Stern-Volmer plot for 6-0 C-H overtone photolysis curved upward at low pressure beginning around 40 Torr. These workers suggested that the curvature resulted from the incomplete collisional deactivation of the MIC activated 8 kcal/mol above the reaction barrier.

Chandler et al.[17] observed unexpected curvature in the Stern-Volmer plots in the vibrational overtone study of *tert*-butyl hydroperoxide induced by excitation of the 5-0 O-H stretch transition. The curvature was explained by invoking a small nonstatistical component to the observed reaction rate. Chuang et al.[18] reported that the nonstatistical channel was more efficient for photolysis into the fifth overtone. Later, Gutow et al.[19] found a low-energy tail of an excited electronic state overlapping the 6-0 transition, while the 5-0 overtone was clear from any electronic contribution. Chandler and Miller performed a theoretical analysis using a master equation formalism in order to simulate the experimental plots in the *tert*-butyl hydroperoxide experiment.[20] Although they could not explain the curvature observed, they did find low-pressure curvature in their computer-generated plots which they attributed to the change in the reactive distribution, $y'(E)$, with pressure. The $y'(E)$ is a function which describes the distribution of the energies of molecules which react. At very low pressures, all the initially activated molecules react so $y'(E)$ is equal to the initial photoactivated distribution before any collisions. On going to higher pressures, this distribution changes until at high pressures the reactive distribution becomes pressure independent. At high pressures, the Stern-Volmer plot is a straight line with a slope different from that at low pressure.

Snavely et al.[21] reinvestigated the isomerization of MIC to determine collisional deactivation parameters using vibrational overtone activation. The isomerization yield depended markedly on the collision partner for the 5-0 and 6-0 overtone vibrational levels even though the single-collision deactivation approximation was expected to have its greatest validity for activation close to the barrier. It was found that the deactivation of vibrationally excited MIC by collision with pure MIC was more rapid than with C_3H_6, SF_6, or Ar. The average energy transferred per collision, $\langle \Delta E \rangle_d$, was calculated by a master equation simulation of the experimental data, using a single-exponential down-transfer probability function to describe the collision dynamics. The theoretical Stern-Volmer plots determined in the work of Miller and Chandler[22] and Snavely et al.[21] exhibit curvature at low pressures. The calculated plot for the fourth overtone curves in a negative direction while the plot for the fifth overtone curves

(1) Crim, F. F. *Annu. Rev. Phys. Chem.* **1984**, *35*, 657.
(2) Reisler, H.; Wittig, C. *Annu. Rev. Phys. Chem.* **1986**, *37*, 307.
(3) Henry, B. R. *Acc. Chem. Res.* **1977**, *10*, 207.
(4) Henry, B. R. *Vib. Spectra Struct.* **1981**, *10*, 269.
(5) Quack, M. *Annu. Rev. Phys. Chem.* **1990**, *41*, 839.
(6) Schneider, F. W.; Rabinovitch, B. S. *J. Am. Chem. Soc.* **1962**, *84*, 4215.
(7) Chan, S. C.; Rabinovitch, B. S.; Bryant, J. T.; Spicer, L. D.; Fujimoto, T.; Lin, Y. N.; Pavlou, S. P. *J. Phys. Chem.* **1970**, *74*, 3160.
(8) Maloney, K. M.; Rabinovitch, B. S. In *Isonitrile Chemistry*; Ugi, I., Ed.; Academic Press: New York, 1971; Chapter 3.
(9) Robinson, P. J.; Holbrook, K. A. *Unimolecular Reactions*; Wiley-Interscience: New York, 1972.
(10) Gilbert, R. G.; Smith, S. C. *Theory of Unimolecular and Recombination Reactions*; Blackwell Scientific: Oxford, 1990.
(11) Harris, H. H.; Bunker, D. L. *Chem. Phys. Lett.* **1971**, *11*, 433.
(12) Bunker, D. L.; Hase, W. L. *J. Chem. Phys.* **1973**, *59*, 4621; *J. Chem. Phys.* **1978**, *69*, 4711.
(13) Bunker, D. L.; Hase, W. L. *J. Chem. Phys.* **1978**, *69*, 4711.
(14) Reddy, K. V.; Berry, M. J. *Chem. Phys. Lett.* **1977**, *52*, 111.
(15) Reddy, K. V.; Berry, M. J. In *Advances in Laser Chemistry*; Zewail, A. H., Ed.; Springer: Berlin, 1978; pp 48-61.
(16) Reddy, K. V.; Berry, M. J. *Faraday Discuss. Chem. Soc.* **1979**, *67*, 188.
(17) Chandler, D. W.; Farneth, W. E.; Zare, R. N. *J. Chem. Phys.* **1982**, *77*, 4447.
(18) Chuang, M.-C.; Baggott, J. E.; Chandler, D. W.; Farneth, W. E.; Zare, R. N. *Faraday Discuss. Chem. Soc.* **1983**, *71*, 301.
(19) Gutow, J. H.; Klenerman, D.; Zare, R. N. *J. Phys. Chem.* **1988**, *92*, 172.
(20) Chandler, D. W.; Miller, J. A. *J. Chem. Phys.* **1984**, *81*, 455.
(21) Snavely, D. L.; Zare, R. N.; Miller, J. A.; Chandler, D. W. *J. Phys. Chem.* **1986**, *90*, 3554.
(22) Miller, J. A.; Chandler, D. W. *J. Chem. Phys.* **1986**, *85*, 4502.

0022-3654/92/2096-2576$03.00/0

in a positive direction. The curvature can once again be understood by observing the pressure dependence of the reactive distribution, $y'(E)$. However, unlike the case for *tert*-butyl hydroperoxide, the direction of the curvature was different for the fourth and fifth overtone excitation. The positive curvature obtained for the 6–0 transition results from the decrease in the reactive distribution mean energy with pressure. The negative curvature obtained for the 5–0 results from the increase in the mean energy of the reactive distribution with increasing pressure. This increase in the mean energy is a consequence of the position of the activation barrier as described more fully under Discussion.

Snavely et al.[21] found the rates of photoisomerization to be increasingly more difficult to measure at low pressures so that the region from 1 to 20 Torr was not studied. The experimental plots curved at low pressures for both overtones; however, the direction of the experimental curvature was opposite to that found theoretically. Because of the uncertainty in the low-pressure data, the direction and magnitude of the experimental curvature could not be verified in the earlier work. We report the observation of the experimental low-pressure curvature using improved analytical procedures.

Recently, Segall and Zare[23] reported that the unimolecular rate coefficient for the photoisomerization of allyl isocyanide, excited to various wavelengths within the rotational band contour of the $5\nu_{C-H}$ and $6\nu_{C-H}$ overtone transitions, exhibits a nonmonotonic behavior with the excitation energy at room temperature. This was explained by a model which assumes an inhomogeneously broadened band shape of the overtones by the presence of vibrational "hot bands". In this model, the molecules have different amounts of initial thermal energy across the overtone band. The "hot band" inhomogeneous broadening model represents an alternative explanation rather than "nonstatistical" effects, which was indicated in previous work by Reddy and Berry.[24]

In allyl isocyanide there are three types of C–H oscillators giving rise to the overtone spectrum. These different C–H stretch overtone transitions overlap at each quantum level; consequently, the separation of vibrational contributions is difficult. Due to these complications, any rotational effects could not be investigated. For methyl isocyanide, with only a single methyl C–H oscillator, the interpretation of the hot band model is simplified. In addition, as was shown for the small molecules, H_2O_2[25] in supersonic jet cooling experiments, and CH_4[26] cooled to 77 K, the width of the band contour involves substantial inhomogeneous broadening. Therefore, we have selected excitation wavelengths within the $5\nu_{C-H}$ and $6\nu_{C-H}$ overtone regions of methyl isocyanide to check the inhomogeneous broadening model. We found that the reaction rate increases monotonically with excitation energy and there is no contribution of hot bands to the photoisomerization reaction.

Experimental Section

Methyl isocyanide (MIC) was synthesized by dehydration of *N*-methyl-formamide.[27] Gas samples of MIC at known pressure (0.1–160 Torr) were photolyzed inside the cavity of a CW dye laser, in a Pyrex sample cell (22.5-cm length, 1.3-cm inside diameter) outfitted with two Brewster angle quartz windows. In order to keep the product yield always ~2% so that absolute quantitatitve yields can be calculated, the samples were photolyzed for time periods ranging from 10 to 40 min, depending on the sample pressure and photolysis wavelength. A Spectra Physics Series 200 argon ion laser was used to pump a Spectra Physics Model 375 B continuous-wave broad-band dye laser. The dye laser was tuned to the required wavelength using a motor-driven three-plate birefringent filter with a resolution of ~2 cm^{-1}. Rhodamine 6G and Pyridine 2 dyes were used in the dye laser for the 6–0 C–H (621.4 nm) and the 5–0 C–H (726.6 nm) overtones, respectively. Wavelengths were measured using a Spex 1401 double monochromator. The Model 815 power meter of Newport Corporation was used to monitor the output power of the dye laser during photolysis to ensure intracavity power stability. Sample pressures were measured using a Datamatrics Type 1400 electronic manometer with a Type 590 series integral Barocel pressure transducer.

After photolysis, the product yield was measured with a Hewlett-Packard 5890 gas chromatograph equiped with a flame ionization detector and 3392A integrator. The sample components, methyl isocyanide and acetonitrile, were completely separated with a 12 ft × $^1/_8$ stainless steel column packed with Chromosorb 104, 80/100 mesh (Alltech Associates). The column temperature maintained at 150 °C with a He carrier gas flow rate of 30 mL/min. Retention times of 9 and 15 min were obtained for MIC and AN, respectively.

Methyl isocyanide sticks to all surfaces, including the glass sample cell and the stainless steel sampling six-port valve and loop. In order to account for this process, a careful analysis procedure was developed. The method of filling the photolysis cell and introducing the sample to the GC column was exactly reproduced for each experiment. The photolysis cell was filled with MIC (150 Torr) and "seasoned" for 5 days. MIC vapor was expanded from the liquid sample holder to the photolysis cell through the vacuum line to obtain gas pressure around the desired pressure. The pressure final reading was taken after waiting 0.5 h, when the change in the pressure become insignificant. The irradiated gas sample was then condensed onto the GC sampling loop by liquid nitrogen for 15 min and injected cold into the column. This procedure (condensing and injection) was repeated at least two times until no more sample was detected. The sum of these three areas was used to calculate the percent product yield. The entire sample was condensed and injected if the pressure was lower than 40 Torr. In order to prevent saturating the GC column and detector, samples with higher pressures were expanded into the sampling loop for 5 min and only this expanded part (~1:5) was condensed and injected as before. The method was checked by injecting a known ~2% gas mixture of AN in MIC at different pressures to give an error of ~1%. Samples of the MIC diluted in Ar in a 1:25 ratio were prepared for each pressure directly in the photolysis cell: MIC vapor was first expanded into the photolysis cell as described before for pure MIC and then the Ar gas, which is stored in a sampling bulb connected to the vacuum line, was introduced to get the correct ratio at the specific pressure. By this we assure that the diluted mixtures have the same composition in the different pressures.

Some of the points were repeated three times in order to estimate the standard deviation. For the fourth overtone the typical error is ~2% while for the fifth overtone it is ~3%. No dark reaction was observed for pure MIC and MIC in Ar without irradiation.

Results

a. Stern–Volmer Analysis. For the vibrational overtone activation experiment, the Stern–Volmer treatment has been used repeatedly.[14] In the simple mechanism (with only one reaction step)

$$A + h\nu \xrightarrow{k_a} A^* \quad \text{photoactivation} \tag{1}$$

$$A^* + M \xrightarrow{k_d} A + M \quad \text{collisional deactivation} \tag{2}$$

$$A^* \xrightarrow{k(\epsilon)} P \quad \text{unimolecular reaction} \tag{3}$$

a steady-state concentration of the activated molecules A^* is assumed and the inverse apparent rate of reaction is plotted against the total pressure for a chosen excitation frequency according to

$$k_{ap}^{-1}[h\nu] = k_a^{-1} + k_d k(\epsilon)^{-1} k_a^{-1}[M] \tag{4}$$

where k_{ap} is the product apparent rate of reaction, k_a is the rate of photoactivation, k_d is the collisional deactivation rate constant,

(23) Segall, J.; Zare, R. N. *J. Chem. Phys.* **1988**, *89*, 5704.
(24) Reddy, K. V.; Berry, M. J. *Chem. Phys. Lett.* **1979**, *66*, 223.
(25) Butler, L. J.; Ticich, T. M.; Likar, M. D.; Crim, F. F. *J. Chem. Phys.* **1986**, *85*, 2331.
(26) Scherer, G. L.; Lehmann, K. K.; Klemperer, W. *J. Chem. Phys.* **1984**, *81*, 5319.
(27) Schuster, R. E.; Scott, J. E.; Casanova, J., Jr. *Organic Syntheses*; Wiley: New York, 1973; Collect. Vol. V, p 772.

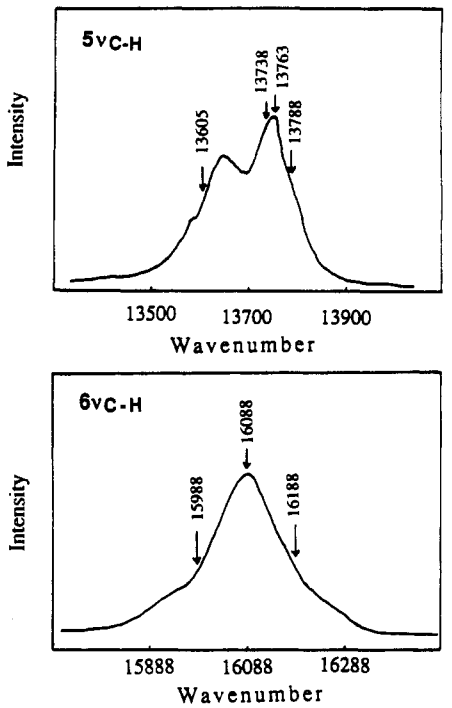

Figure 1. Vibrational overtone absorption spectrum of gaseous methyl isocyanide for the $5\nu_{C-H}$ and $6\nu_{C-H}$ overtones.

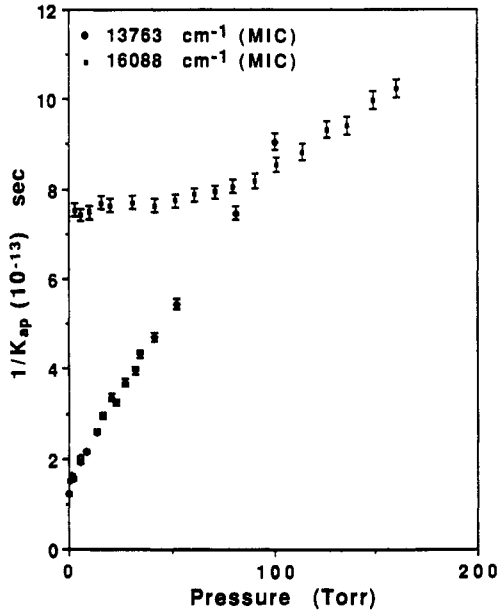

Figure 2. Stern–Volmer plots for photolysis of pure MIC at the $5\nu_{C-H}$ (13 763 cm^{-1}) and $6\nu_{C-H}$ (16 088 cm^{-1}) overtones.

$k(\epsilon)$ is the unimolecular rate coefficient and $[h\nu]$ is the intracavity photon number density. In the simple "strong collider approximation", the Stern–Volmer plot should be a straight line for all pressure regions. The slope of this line yields the ratio of the collisional deactivation rate to the unimolecular rate coefficient, $k_d/k(\epsilon)$, while from the intercept, the photoactivation rate k_a can be obtained. k_a can be calculated independently by the equation

$$k_a = \sigma(\nu)c \tag{5}$$

where $\sigma(\nu)$ is the absorption cross section at the photolysis frequency and c is the speed of light. The photon number density is determined at each wavelength using the relation

$$[h\nu] = 2(5.04 \times 10^{14})\lambda p/cTA_{eff} \tag{6}$$

where λ is the photolysis wavelength (in Å), T is the transmittance of the dye laser end mirror at the photolysis wavelength, c is the speed of light, A_{eff} is the effective cross sectional area (in cm^2)

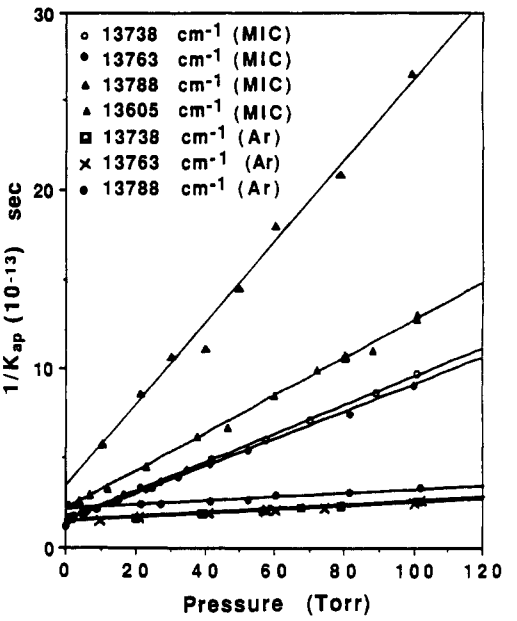

Figure 3. Stern–Volmer plots for photolysis of pure MIC and MIC diluted with Ar (1:25) at several wavelengths across the $5\nu_{C-H}$ overtone region.

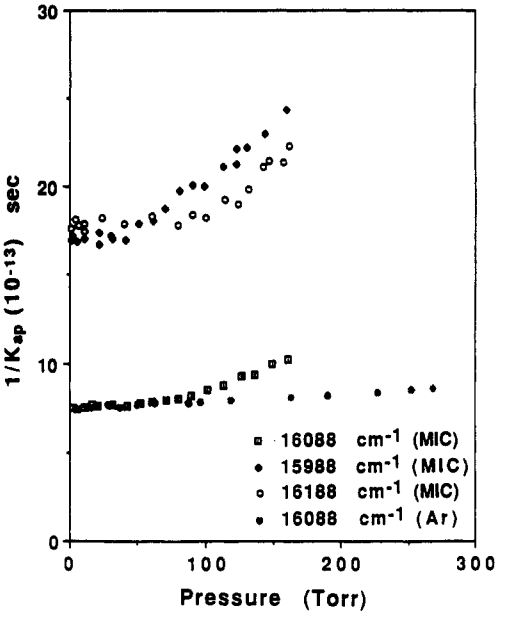

Figure 4. Stern–Volmer plots for photolysis of MIC and MIC diluted in Ar (1:25) at several wavelengths across the $6\nu_{C-H}$ overtone region.

of the cell defined as the cell volume divided by the cell length, and p is the extracavity power (in W), during photolysis.[16,28]

b. Photoisomerization Results. The photolysis wavenumbers chosen for investigation are shown in Figure 1. Four photolysis energies within the 5–0 band contour and three within the 6–0 contour were selected. The 5–0 transition peak maximum occurs at 13 763 cm^{-1}. Photolysis experiments were performed on this peak, 25 cm^{-1} to the red and 25 cm^{-1} to the blue. Because the 5–0 contour is not symmetric, we chose one additional energy shifted 158 cm^{-1} to the red. For the 6–0 photolysis, the peak maximum at 16 088 cm^{-1} and additional energies 100 cm^{-1} to the red and blue were chosen.

Figure 2 presents the Stern–Volmer plots for MIC photoisomerization excited at the $5\nu_{C-H}$ (13 763 cm^{-1}) and $6\nu_{C-H}$ (16 088 cm^{-1}) overtone transitions. The fourth overtone excitation shows negative curvature (decreasing slope with increasing pressure) at low pressure. A positive curvature (increasing slope with increasing

(28) Chuang, M.-C.; Zare, R. N. *J. Chem. Phys.* **1985**, *82*, 4791.

TABLE I: Absorption Cross Sections from the $5\nu_{C-H}$ and $6\nu_{C-H}$ Overtone Region of MIC

overtone transition	ν, cm^{-1}	collider gas	σ,[a] mb	σ,[b] mb
5–0	13605	MIC	1013	550
	13738		2148	1168
	13763		2215	1200
	13788		1542	758
5–0	13738	Ar	2212	
	13763		2284	
	13788		1555	
6–0	15988	MIC	227	55
	16088		517	120
	16188		230	55
6–0	16088	Ar	447	

[a] Cross sections from Stern–Volmer intercepts. [b] Spectroscopic cross sections taken from ref 16.

TABLE II: Specific Reaction Rate Constants Derived from the Experimental Stern–Volmer Photolysis Plots at Different Excitation Energies

overtone transition	ν, cm^{-1}	collider gas	$k(\epsilon)$, s^{-1}
5–0	13605	MIC	$(2.85 \pm 0.06) \times 10^8$
	13738		$(3.87 \pm 0.08) \times 10^8$
	13763		$(3.94 \pm 0.08) \times 10^8$
	13788		$(4.09 \pm 0.08) \times 10^8$
6–0	15988	MIC	$(5.0 \pm 0.2) \times 10^9$
	16088		$(5.7 \pm 0.1) \times 10^9$
	16188		$(6.6 \pm 0.2) \times 10^9$

pressure) is seen for the fifth overtone.

Figures 3 and 4 show Stern–Volmer plots for the photolysis of pure MIC and MIC diluted in argon at several wavelengths selected from across the $5\nu_{C-H}$ and $6\nu_{C-H}$ regions, respectively. Only data above 10 and 40 Torr were considered in fitting the $5\nu_{C-H}$ and $6\nu_{C-H}$ overtone regions, respectively. The extrapolated intercepts for these plots approximately followed the change in absorption intensity at the different wavelengths across the rotational band contours. Table I gives the absorption cross sections obtained from our experimental Stern–Volmer intercepts and the measured spectroscopic cross sections (taken from ref 16). The cross-section values we obtained are a factor of about 2–4 higher, but the ratios of the cross sections for the different wavelengths are still the same.

The unimolecular rate coefficient, $k(\epsilon)$, values determined by linear regression fits to the experimental data, are tabulated in Table II. The rate coefficients were obtained from the slopes and intercepts extrapolated from the linear high-pressure data only. In order to determine the $k(\epsilon)$, the value of k_d must be calculated using either the hard-sphere, Lennard-Jones or Stockmayer collision model. The Stockmayer potential collision parameters (appropriate for polar collision partners) were used in this work. For MIC–MIC, the collision frequency is 1.99×10^7 Torr^{-1} s^{-1} and for MIC–Ar is 9.58×10^6 Torr^{-1} s^{-1}, as obtained in ref 21. In every case, $k(\epsilon)$ increases monotonically with increasing excitation energy even within the individual band contours.

Discussion

a. Curvature in Stern–Volmer Plots at Low Pressure. Stern–Volmer analysis of photochemical kinetics is a well-known technique for determining rate constants.[29] The underlying mechanistic assumption involves the decay of the excited state of interest through competition between reaction and collisional quenching. The yield versus concentration (pressure) plot is linear if the rate constants do not depend on concentration. For vibrational overtone activation, the slope of the Stern–Volmer plot is proportional to the ratio $k_d/k(\epsilon)$. In this case, the experimental $k_d/k(\epsilon)$ value is an average over the population distribution of activated molecules and, therefore, depends on the pressure.[22]

(29) Turro, N. J. *Modern Molecular Photochemistry*; Benjamin/Cummings: Reading, MA, 1978; Chapter 8.

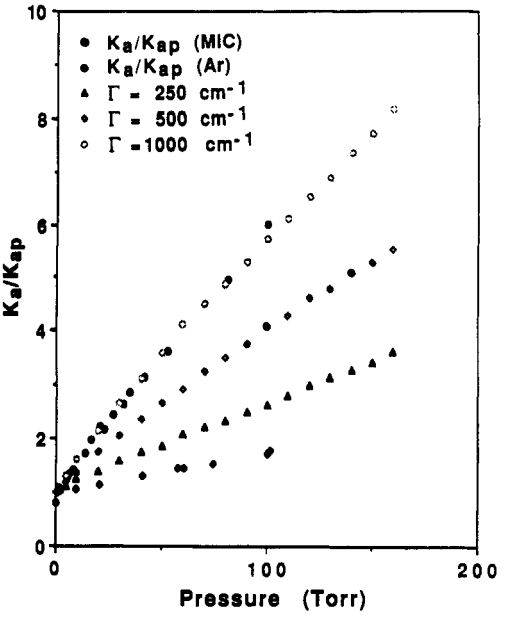

Figure 5. Stern–Volmer plots: simulated and experimental data for the $5\nu_{C-H}$ overtone.

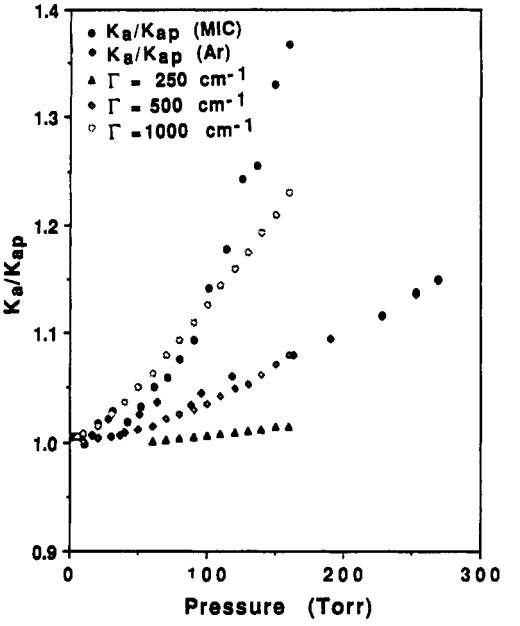

Figure 6. Stern–Volmer plots: simulated and experimental data for the $6\nu_{C-H}$ overtone.

Figures 5 and 6 show the experimental data scaled to represent the yield for the photolysis at the fourth and fifth overtones, respectively, along with the theoretical curves taken from the work in ref 21. The scaled Stern–Volmer plot can be obtained by rewriting eq 4 as

$$k_a/k_{ap} = 1 + \{k_d/k(\epsilon)\}[M] \quad (7)$$

In this reduced Stern–Volmer equation, the plots are normalized to the change in the absorption intensity at the photolysis wavelengths. The theoretical curves are those calculated using the master equation model described in the work of Miller and Chandler[22] and Snavely et al.[21] The curves were obtained using the "300 model" parameters given by Rabinovitch,[8] with an isomerization barrier height 200 cm^{-1} higher than that of the 300 model. An exponential down energy-transfer probability function was assumed for calculating $\langle \Delta E \rangle_d$, the average amount of energy transferred per collision. Curves labeled with different Γ correspond to plots where Γ is the average amount of energy transferred in a deactivating collision. The very small modification of the

300 model barrier was necessary in order to fit the experimental data. It can be seen that the direction of the low-pressure curvature of the experimental and theoretical curves is the same. In addition, the overall magnitude of the curvature for the simulated plots agrees with the experimental curvature.

In the photoactivation process a distribution of total energies in the activated molecules is produced. In the overtone excitation experiments it is usually assumed that this initial distribution is the same as the room temperature Boltzmann distribution displaced by the energy of the photon. Following the discussion of Miller and Chandler,[22] the curvature can be understood by observing changes in the distribution of activated molecules. This reactive distribution, $y'(E)$, describes the energy distribution of activated molecules which become product. At very low pressures $[k_dP \ll k(\epsilon)]$, the reactive distribution function is equal to the initial photoactivated distribution, $y'(E) = y^0(E)$. That is, all of the initially activated molecules react before any collisions occur. For the fourth overtone, as the pressure increases, collisional deactivation moves many of the less energetic activated molecules below the activation barrier, shifting the reactive distribution to higher energies. This happens because of the proximity of the reaction barrier and the energy of the fourth overtone. As the reactive distribution shifts to higher energy the product yield is higher, resulting in negative curvature in the Stern–Volmer plot. For excitation into the fifth overtone, which is approximately 8 kcal/mol above the activation barrier, the situation is different. Here the reactive distribution shifts to lower energies with pressure. This is the natural behavior that we would expect from collisional deactivation. The positive curvature of the Stern–Volmer plot results from the decreased yield as $y'(E)$ shifts to lower energies. At much higher pressures $[k_dP \gg k(\epsilon)]$, the reactive distribution does not depend on the pressure at all and a straight line is expected for the Stern–Volmer plot.

The curvature is sensitive to the height of the activation barrier, the collisional deactivation efficiency of the collider gas, and the magnitude of the unimolecular rate coefficient for reaction.[21] This type of curvature will be observed when the unimolecular rate coefficient for the reaction is comparable in magnitude to the collisional deactivation rate. The observation of the curvature experimentally depends only on the appropriate choice of pressure for each reaction.

The isomerization reaction of methyl isocyanide is the only reaction using overtone activation where this experimental curvature has been observed. According to our understanding, no curvature should have been observed in the pressure range studied in these other reactions. For example, for the isomerization of cyclobutene,[30] the measured unimolecular rate coefficient was 0.40×10^8 and 0.91×10^8 s^{-1} for the two different C–H stretches in the fourth overtone excitation and 4.90×10^8 and 8.20×10^8 s^{-1} for the fifth overtone. The curvature would be expected in the pressure range of 6–12 Torr; however, a careful low-pressure study has not been done.[30,31] The strongest peak in the fourth overtone region is approximately 4.4 kcal/mol above the activation barrier and the fifth overtone is 10.9 kcal/mol so it should be possible to observe the change in curvature (from negative to positive) as the internal energy of the activated molecules is increased. For methylcyclopentadiene,[32] where a unimolecular rate coefficient of 1.3×10^7 s^{-1} has been measured for the 13 221-cm^{-1} excitation of the fourth overtone, the curvature should occur at even lower pressures around 0.5–1 Torr. Since the fourth overtone transition is 10.8 kcal/mol above the activation barrier, a positive curvature is expected, typical of excitation above the threshold.

b. Collisional Deactivation Efficiency. In the Stern–Volmer analysis of the data obtained in overtone excitation experiments, the collisional deactivation process is usually treated in the single-collision approximation. By this approximation it is assumed that one collision of the excited molecule with an unexcited partner molecule is sufficient to remove enough energy, preventing reaction. Therefore, the collisional deactivation rate constant is the collision frequency, $k_d = Z$. However, it has been shown before[21] that this approximation fails even in cases where the excitation energy is very close to the reaction barrier, and k_d should be given by the product of

$$k_d = \gamma Z \tag{8}$$

where γ is the collision efficiency factor. The experimental γ can be derived from the Stern–Volmer plots, by assuming that the $k(\epsilon)$ is the same for the MIC–MIC and MIC–Ar cases at a particular excitation energy (Figures 3 and 4). The relative collision efficiencies between these two systems can be deduced from the ratio of the slopes for the two curves as follows:

$$\frac{\text{slope}_{Ar}}{\text{slope}_{MIC}} = \frac{[\gamma Z/k_a k(\epsilon)]_{Ar}}{[\gamma Z/k_a k(\epsilon)]_{MIC}} = \frac{[\gamma Z]_{Ar}}{[\gamma Z]_{MIC}} \tag{9}$$

where the collisional deactivation efficiency of MIC is taken as 1. This is tabulated in Table III combined with the thermal activation result.[7]

TABLE III: Relative Collision Efficiency for MIC–MIC and MIC–Ar

overtone transition	ν, cm^{-1}	rel collision efficiency
5–0	13 738	0.30 ± 0.01
	13 763	0.31 ± 0.02
	13 788	0.24 ± 0.01
6–0	16 088	0.33 ± 0.02
thermal data[a]		0.14

[a] Reference 7.

It can be seen that the relative efficiency in the overtone photoactivation experiment is higher by a factor of ~2 relative to the thermal results. This can be understood by considering the basic difference between the two activation methods. In thermal activation, the colliding partner molecule contains thermal vibrational energy according to the thermal distribution at the specific temperature. However, for overtone photoactivation, the collider molecule is relatively "cold", containing only room temperature thermal energy as determined by the Boltzmann distribution. It is reasonable that the collisional deactivation process would be more efficient with the "colder" molecule, so the collisional deactivation rate should be higher in the overtone photoactivation experiment relative to the thermal one. However, the increase in efficiency is not the same for the pure collider and the argon cases. Because we can only measure a ratio, it is impossible to say whether the MIC–MIC collisions have increased less in the overtone activation case or whether the Ar–MIC collisions increased more. Comparing the fourth and fifth overtones, the collisional deactivation efficiency is higher for the fifth overtone, where this difference in internal energy between the two colliding partners is even larger.

From a comparison of the experimental and theoretical curves, as shown in Figures 5 and 6, the average amount of energy transferred per collision for methyl isocyanide is around 1000 cm^{-1}. This value is lower than the previously reported value of 1375 cm^{-1}.[21] For argon as the collider gas, the average amount of energy transferred per collision is lower than 250 cm^{-1} for the fourth overtone and around 500 cm^{-1} for the fifth overtone. The theoretical curves were originally calculated so that the same amount of energy, $\langle \Delta E \rangle_d$, was transferred for methyl isocyanide for both overtones. Taking the average for argon indicated that argon transfers around 350 cm^{-1}. This value is higher than previously measured but consistent with our understanding that argon has a higher collisional deactivation efficiency in the vibrational overtone activation than in thermal experiments.

c. Overtone Transition Broadening Mechanisms. At room temperature, the 5–0 and 6–0 C–H vibrational overtone transitions in gaseous methyl isocyanide are over 100 cm^{-1} wide. The absorption contours have contributions from both the rotational and vibrational absorptions, as well as homogeneous broadening. As mentioned before, the width of the band contour for small mol-

(30) Jasinski, J. M.; Frisoli, J. K.; Moore, C. B. *J. Chem. Phys.* **1983**, *79*, 1312.
(31) Baggott, J. E.; Law, D. W. *J. Chem. Phys.* **1986**, *85*, 6475.
(32) Jasinski, J. M.; Frisoli, J. K.; Moore, C. B. *J. Phys. Chem.* **1983**, *87*, 2209.

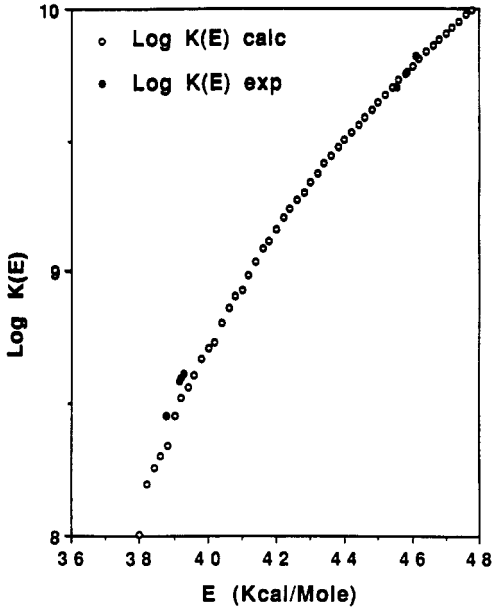

Figure 7. Calculated RRKM rate constant for MIC isomerization, with the experimental photoisomerization rate constants.

ecules (H_2O_2,[25] CH_4[26]) has been shown to involve substantial inhomogeneous broadening. In other experiments,[33] slightly cooling larger molecules (ethylene, ethane, propyne, allene, propane, cyclopropane, dimethyl ether, isobutane) to temperatures between 143 and 189 K did not dramatically change the band contours. Methyl isocyanide possesses a low-frequency bending mode which is populated at room temperature. This low-frequency mode is envisioned as the reaction coordinate in the isomerization reaction to produce acetonitrile. The overtone absorption for molecules containing one quantum of bend will absorb on the red side of the overtone feature due to anharmonicity. Thus photolysis on the red side of the 5–0 or 6–0 overtone transition might selectively excited molecules which already contain internal vibrational energy. In the infrared the high J'' states absorb at the low- and high-energy sides of the band contour. Although the rotational analysis of vibrational overtone transitions for molecules as large as MIC has not been accomplished, we believe the same will be true for the overtone spectra. This could lead to a nonmonotonic variation of the specific rate constants, $k(\epsilon)$, with the excitation energy, as obtained in the allyl isocyanide case.[23]

Figure 7 presents a plot of the RRKM calculated $k(\epsilon)$ along with the experimental values taken from Table II for MIC in both overtone transitions. The Hase–Bunker RRKM program[34] was used for the calculation. The program was run with the following options: (1) adiabatic rotations and harmonic vibrations, (2) direct counting for the sum of states in the critical configuration and semiclassical counting in the reactant, (3) prescribed critical configuration, and (4) a reaction path degeneracy of 3 and a critical energy of 37.85 kcal/mol, as given in ref 8. The vibrational and rotational parameters of the "300 model" for MIC suggested by Rabinovitch[8] were used.

As can be seen from Figure 7, the experimental $k(\epsilon)$ agree with the calculated values and increase with increasing excitation energy. This behavior is in contrast to the previous results obtained for allyl isocyanide,[23] indicating that the vibrational and rotational contribution to the width of the broad overtone feature in methyl isocyanide is small; i.e., the homogeneous broadening mechanism is dominant. However, a low-temperature spectrum of the overtone transitions is still needed to confirm the above conclusion.

Conclusions

The vibrational overtone photoactivation of gaseous methyl isocyanide into the fourth and fifth C–H vibrational overtone states has been studied at pressures from 0.5 to 160 Torr. Photolysis wavelengths across the rotational band contours were selected, and the measured $k(\epsilon)$ values were compared to those for photolysis on the absorption peak. The measured $k(\epsilon)$ values increased with increasing excitation energy and compared well to the calculated RRKM $k(\epsilon)$ values. The Stern–Volmer plots curve at low pressures. This curvature results from the narrow energy distribution of the activated molecules in the vibrational overtone activation experiment and the proximity of the photoactivation energy to the activation barrier. Argon and methyl isocyanide were used as collider gases for both overtone transitions. The collisional deactivation efficiency of Ar, derived from the change in the Stern–Volmer slopes is greater than in thermal activation experiments.

Registry No. MIC, 593-75-9; AN, 75-05-8.

(33) Crofton, M. W.; Stevens, C. G.; Klenerman, D.; Gutow, J. H.; Zare, R. N. *J. Chem. Phys.* **1988**, *89*, 7100.

(34) *Quantum Chemistry Program Exchange No. 234*, Chemistry Department, Indiana University, Bloomington, IN.